




Molecular characterization of *HDAC8* deletions in individuals with atypical Cornelia de Lange syndrome

Maria Helgeson¹ · Jennifer Keller-Ramey¹ · Amy Knight Johnson¹ · Jennifer A. Lee² · Daniel B. Magner³ · Brett Deml¹ · Jacea Deml¹ · Ying-Ying Hu¹ · Zejuan Li¹ · Kirsten Donato¹ · Soma Das¹ · Rachel Laframboise⁴ · Sandra Tremblay⁴ · Ian Krantz⁵ · Sarah Noon⁵ · George Hoganson⁶ · Jennifer Burton⁶ · Christian P. Schaaf^{7,8}  · Daniela del Gaudio¹

Received: 24 July 2017 / Revised: 2 October 2017 / Accepted: 25 October 2017 / Published online: 26 December 2017
© The Japan Society of Human Genetics 2018

Abstract

Cornelia de Lange syndrome (CdLS) is a rare neurodevelopmental syndrome for which mutations in five causative genes that encode (*SMC1A*, *SMC3*, *RAD21*) or regulate (*NIPBL*, *HDAC8*) the cohesin complex, account for ~70% of cases. Herein we report on four female Subjects who were found to carry novel intragenic deletions in *HDAC8*. In one case, the deletion was found in mosaic state and it was determined to be present in ~38% of blood lymphocytes and in nearly all cells of a buccal sample. All deletions, for which parental blood samples were available, were shown to have arisen de novo. X-chromosome inactivation studies demonstrated marked skewing, suggesting strong selection against the mutated *HDAC8* allele. Based on an investigation of the deletion breakpoints, we hypothesize that microhomology-mediated replicative mechanisms may be implicated in the formation of some of these rearrangements. This study broadens the mutational spectrum of *HDAC8*, provides the first description of a causative *HDAC8* somatic mutation and increases the knowledge on possible mutational mechanisms underlying copy number variations in *HDAC8*. Moreover our findings highlight the clinical utility of considering copy number analysis in *HDAC8* as well as the analysis on DNA from more than one tissue as an indispensable part of the routine molecular diagnosis of individuals with CdLS or CdLS-overlapping features.

Electronic supplementary material The online version of this article (<https://doi.org/10.1038/s10038-017-0387-6>) contains supplementary material, which is available to authorized users.

✉ Daniela del Gaudio
ddelgaudio@bsd.uchicago.edu

- ¹ Department of Human Genetics, University of Chicago, Chicago, IL, USA
- ² Greenwood Genetic Center, Greenwood, SC, USA
- ³ IAM Scientific, Inc, Greenville, SC, USA
- ⁴ CHU de Quebec, CHUL, Quebec, QC, Canada
- ⁵ Division of Human Genetics, The Children's Hospital of Philadelphia, Philadelphia, PA, USA
- ⁶ University of Illinois College of Medicine, Peoria, IL, USA
- ⁷ Department of Molecular and Human Genetics, Baylor College of Medicine, Houston, TX, USA
- ⁸ Jan and Dan Duncan Neurological Research Institute, Texas Children's Hospital, Houston, TX, USA

Introduction

Cornelia de Lange syndrome (CdLS; OMIM# 122470, 300590, 610759, 300882, and 614701) is a genetically heterogeneous disorder characterized by distinctive facial features, hirsutism, upper limb anomalies, growth retardation, and intellectual disabilities. Classic CdLS is associated with a severe phenotype with profound growth and neurodevelopmental delays, striking dysmorphic craniofacial features and reduction defects of the upper extremities ranging from complete absence of the forearms to oligodactyly [1]. Individuals with milder, atypical phenotype have less severe growth, cognitive and limb involvement, but often have facial features consistent with CdLS [2]. An estimated 60% of clinically well-defined CdLS cases harbor a *de novo* heterozygous mutation in the cohesin loader gene *NIPBL* [3]. About 10% of the patients carry a variant in the structural components of the chomatin-associated complex cohesin, *SMC1A* [4, 5], *SMC3* [4], or *RAD21* [6]. These patients present with a milder or less typical phenotype. A fifth CdLS gene, *HDAC8*, encodes a

vertebrate SMC3 deacetylase that has roles in catalyzing the deacetylation of SMC3 as well as in recycling of cohesin for the next cell cycle [7].

Recent studies indicate that a significant proportion of CdLS individuals, in whom mutations in the five-known CdLS-associated genes were excluded by conventional Sanger sequencing performed on DNA isolated from blood, harbor somatic mutations in *NIPBL* in DNA derived from buccal mucosa [8–10]. Among the viable explanations are, the limited sensitivity of Sanger sequencing for detection of mosaicism and the loss of mutations in leukocytes due to reversion and leukocyte specific selection against mutant cells [8, 11]. Mosaicism has also been reported in *SMC1A* and *SMC3* [8, 12]; however, somatic mosaicism for a mutation in *HDAC8* resulting in a CdLS phenotype has not been previously reported.

To date, 41 different loss-of-function mutations in *HDAC8* including six large deletions and one insertion have been reported [7, 13, 14], the majority of which were shown to have occurred *de novo* [13, 14].

In addition to typical CdLS features, *HDAC8*-patients can also exhibit some distinct features including hypertelorism, a broad or bulbous nasal tip, tooth anomalies, and mosaic patches of hyperpigmented skin [13, 14]. The phenotypic spectrum of *HDAC8*-related CdLS is consistent with *HDAC8* localization on the X chromosome, with males being more severely affected than females. Females, who represent more than two-thirds of reported patients, display variable clinical severity that is heavily influenced by X-inactivation patterns. Most female patients demonstrate complete skewing towards full expression of the normal allele in blood, indicating a strong selection against the mutant allele [13, 14].

Several mechanisms have been proposed for the formation of disease-associated copy number variations (CNVs). Non-allelic homologous recombination (NAHR) is the main mechanism for the formation of recurrent genomic rearrangements by using low-copy repeats as a substrate for recombination [15]. Moreover, non-homologous end joining (NHEJ) and the DNA replication-based mechanisms of fork stalling and template switching (FoSTeS)/microhomology-mediated break-induced replication (MMBIR) [16] have been found to play an important role in the generation of nonrecurrent and complex rearrangements in human diseases [17, 18]. While disease-causing CNVs have been reported in *HDAC8*, the mutational mechanism underlying these rearrangements has not been elucidated.

In this study, we describe the identification of four female Subjects with CdLS-overlapping phenotypes carrying novel intragenic deletions in *HDAC8*, including the first report of somatic mosaicism. Furthermore, we characterized the breakpoint junctions of the deletions to gain insight into the underlying molecular mechanisms of these rearrangements.

Materials and methods

Patients

Over the past 6 years, 126 samples were referred to our laboratory for *HDAC8* deletion/duplication analysis. In all patients, previous testing performed using Sanger sequencing and exon-targeted oligonucleotide array comparative genomic hybridization (array-CGH), had excluded the presence of point mutations and copy number abnormalities in *NIPBL*, *SMC1A*, *SMC3*, and *RAD21* as well as point mutations in *HDAC8*. Genomic DNA was isolated from blood leukocytes on the AutoGenFlex STAR robotic workstation (Autogen, Holliston, MA) following the manufacturer's instructions.

Array comparative genomic hybridization

Deletion and duplication analysis of the *HDAC8* gene was performed using a high resolution, custom-designed, exon-targeted 4×180 K array-CGH platform (Agilent Technologies, Santa Clara, CA). A total of 1811 probes spanned the *HDAC8* gene, with an average resolution of ~ 1 probe/20 bp across the coding regions. Genomic DNA samples of the patients and gender-matched control were processed and co-hybridized onto microarray slides according to the manufacturer recommended procedures (Agilent Technologies). Microarray images were scanned at 2μ resolution and the data was extracted using ImaGene (9.0) and analyzed using the Nexus software (7.1) (BioDiscovery, Hawthorne, CA). The genomic copy number was defined by analysis of the normalized \log_2 (Cy5/Cy3) ratio average of the CGH signal. Regions that reached a threshold of at least -0.32 were considered suspicious for copy number losses consistent with deletions.

Quantitative real-time PCR

Relative quantification of *HDAC8* exon 3 in the DNA isolated from blood and buccal sample of Subject 4 was performed by quantitative real-time PCR with primers HDAC8 ex3 F (5'-TAAGCCTAAAGTGGCCTCCA-3') and HDAC8 ex3 R (5'-CATATTCTATGGAGTCCGGATG'-3'). Analysis was performed using 20 ng of genomic DNA. Reactions were done in triplicate, wherein each target region was co-amplified with an internal control (*PMP22*: NM_000304.2) using the SYBR-Green detection chemistry and the ABI PRISM 7500 sequence detection system (Applied Biosystems, Grand Island, NY). Relative quantification of the target gene was determined by the comparative threshold cycle method ($\Delta\Delta Ct$) [19]. DNA samples from a male and female control with normal *HDAC8* copy

Table 1 Clinical features of the individuals with *HDAC8* deletions identified in this study

	Subject 1	Subject 2	Subject 3	Subject 4
cDNA nomenclature	c.437 + 8999_c.629 + 248del	c.437 + 29302_c.737 + 683delinsCAC	c.628 + 251_737 + 689del	c.165–74_437 + 1785del
Genomic coordinates (GRCh37 [hg19])	chrX:71,709,139_71,778,323	chrX:71,708,032_71,758,483	chrX:71,708,032_71,709,965	chrX:71,785,061_71,788,890
Size of the deletion (Kb)	69	50.3	2.4	2.8
Exons involved	5–6	5–7	7	3–4
Inheritance	<i>De novo</i>	<i>De novo</i>	N/A	<i>De novo</i> (in mosaic state)
X-inactivation ratio	98:2	91:9	91:9	60:40, 82:18 ^a
Age at testing	2 years	7 years	7 years	16 years
Birth growth parameters (SD from mean) ^b				
Length	–2.88 SD	N/A	–4.15 SD	–1.79 SD
Weight	–1.94 SD	–1.55 SD	–2.25 SD	–1.81 SD
Head circumference	N/A	N/A	–3.86 SD	–1.83 SD
Growth parameters at most recent evaluation (standard deviations from mean) ^b				
Age at evaluation	6 years 2 months	10 years 9 months	7 years 2 months	17 years 4 months
Height	–2.37 SD	–2.22 SD	–2.77 SD	–2.47 SD
Weight	–1.89 SD	+ 0.86 SD	–3.13 SD	–3.52 SD
Head circumference	–3.6 SD	–3.11 SD	–5.9 SD	–4.0 SD
Growth				
Microcephaly	+	+	+	+
Short stature	+	+	+	+
Poor weight gain	+	N/A	+	+
Development/neurologic				
Developmental delay	+	+	+	+
Speech problems	Verbal apraxia	Nonverbal	Nonverbal	Selective mutism
Hypotonia	+	N/A	+	–
Craniofacial				
Synophrys	+	+	+	+
Wide nasal bridge	+	+	N/A	+
Bulbous nasal tip	+	+	N/A	+
Smooth philtrum	+	+	N/A	+
Posteriorly rotated ears	+	+	+	–
Musculoskeletal				
Small hands/feet	+	+	+	–
Brachydactyly	+	+	+	+
Cardiovascular				
ASD or VSD	–	+	+	–
Other clinical findings	Perinatal hypoglycemia cutis marmorata	Cleft palate chronic otitis media	Prenatal drug/alcohol exposure perinatal hypoglycemia congenital diaphragmatic hernia hirsutism	Behavioral issues Autism Full lips

^aXCI ratio in the buccal specimen^bStandard deviations (SD) based on CDC Growth Charts

number were used to estimate the approximate proportion of mutant cells in the blood and buccal samples of Subject 4.

HDAC8 breakpoint junction sequence analysis

Breakpoint sequence analysis of the *HDAC8* deletions was performed by PCR primer walking using HotStar Taq polymerase (Qiagen, Germantown, MD). PCR primers were

Fig. 1 Clinical findings in Subject 1 at age 6 years and Subject 2 at age 8 years. **a, b** Facial features of Subject 1, showing synophrys, broad nasal bridge, lowset ears, widely spaced teeth. **c** 2–3 toe syndactyly and **d** brachydactyly in Subject 1. **e** Facial features of Subject 2, showing mild synophrys, wide nasal bridge, bulbous nasal tip. **f** Tapered fingers and brachydactyly in Subject 2 (Color figure online)



designed from the *HDAC8* reference sequence (NM_018486.2) across each deleted region derived from the array-CGH results assuming the most likely rearrangement (Supplementary Table 1). Sequencing products were compared to the *HDAC8* reference sequence using Mutation Surveyor software version 3.01 (SoftGenetics, State College, PA) and breakpoint sequences were aligned manually or using MultAlin (<http://multalin.toulouse.inra.fr/multalin/>) [20].

X-inactivation analysis

X-inactivation (XCI) analysis was performed using a well-characterized assay that measures the methylation status in the 5'UTR of the Androgen Receptor gene of the inactivated X chromosome [21]. X-inactivation patterns were determined by comparing the ratios of amplified DNA products for each allele before versus after digestion. Amplification bias for the smaller alleles is accounted for using an empirically determined correction factor. The following XCI thresholds were used for interpretation: below 80% is considered random X-inactivation, 80–90% is considered moderately skewed, and above 90% is considered highly skewed.

Results

Intragenic deletions in *HDAC8* were identified in four female Subjects (Table 1). Consent for photographs was

obtained for Subjects 1 and 2 (Fig. 1). All Subjects have clinical features similar to those observed in typical CdLS, including non-specific features such short stature (4/4), microcephaly (4/4), poor weight gain (2/4), and more typical CdLS craniofacial features including synophrys (4/4), wide nasal bridge (2/4), smooth philtrum (2/4), and posteriorly rotated ears (3/4). Other findings suggestive of CdLS include cutis marmorata (1/4), hirsutism (1/4), small hands and feet (3/4), and brachydactyly (4/4). A bulbous nasal tip, a feature previously reported to be more typical in CdLS patients with *HDAC8* mutations [13], was reported to be present in Subjects 1 and 2 (Fig. 1). All Subjects exhibited some degree of speech impairment, ranging from verbal apraxia to absent speech. Limb anomalies were not detected in any of the Subjects. In addition, several congenital defects were reported in our patients, including atrial septal defects, cleft palate, and diaphragmatic hernia.

All deletions are novel, range in size from ~2.4 to 70 kb and encompass up to three exons (Fig. 2). One deletion encompassing exons 3 and 4 was found to be in an apparently mosaic state in blood (Subject 4) as the array-CGH data showed a low-level reduction in the Cy5/Cy3 fluorescence log₂ ratio (average probes' log₂ ratio of approximately –0.3) of oligonucleotide probes interrogating these exons. Repeat analysis on DNA obtained from a buccal swab from this individual confirmed the presence of the deletion in a larger proportion of cells (average probes' log₂ ratio of approximately –0.5). Quantitative PCR analysis indicated that, compared to a normal female control, the relative copy number of *HDAC8* exon 3 was 81% in the

blood and 48% in the buccal sample (Fig. 3). This indicates that ~38% of blood lymphocytes contain a deletion of one allele of *HDAC8* and nearly all of the cells in the buccal sample contain the deletion.

The deletions occurred *de novo* in all cases for which parental testing was available (3 out of 4). X-inactivation studies on DNA from blood revealed significant skewing in Subjects 1 to 3. Subject 4, who carried the mosaic deletion, showed a random X-inactivation pattern in blood and moderate skewing in buccal cells (Table 1).

Analysis of the breakpoint regions revealed that for all four breakpoints the distal or proximal ends of the deletions harbored repetitive sequences, including short or long interspersed repeat elements. In addition, breakpoints from each of these individuals showed two to three base-pairs of shared microhomology between proximal and distal reference sequences (Fig. 4). The proximal breakpoint of Subject 1, which maps to a long interspersed repeat element (LINE; *LIPB1*), has a three base-pair microhomology (AAC) at the breakpoint junction (Fig. 4a). The deletion in Subject 2 lies within a short interspersed repetitive element (SINE,

AluSz6) at the proximal breakpoint and has a deletion-insertion of three base-pairs (CAC) and a two base-pair microhomology (CT) at the breakpoint junction (Fig. 4b).

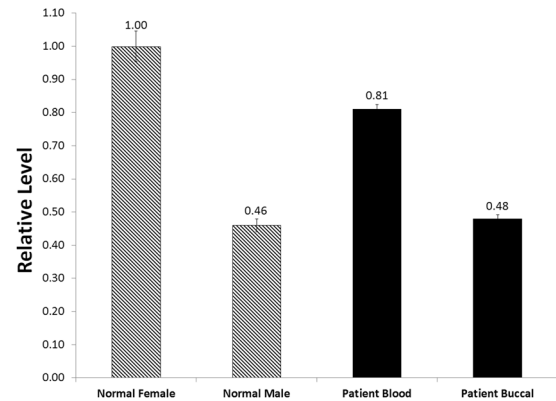


Fig. 3 Estimation of the proportion of mosaicism for the deletion in Subject 4. Relative quantification *HDAC8* exon 3 by qPCR. Normal female and male control (dashed bars) relative to a normal female control; Subject's 4 blood and buccal samples (black bars) relative to a normal female control

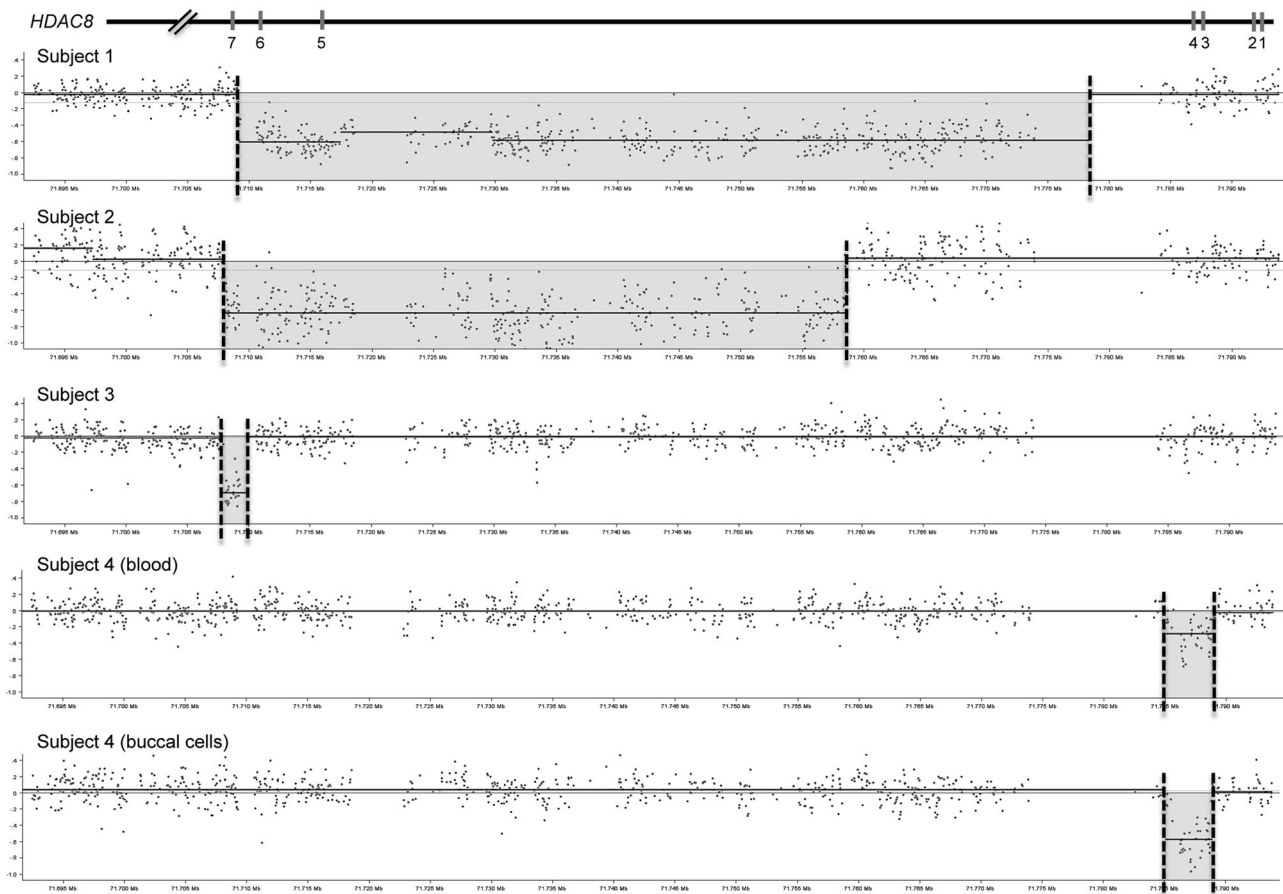


Fig. 2 Array-CGH results for each Subject. *HDAC8* deletions are highlighted in red and evidenced by the reduced log₂ fluorescence ratios. The approximate positions of *HDAC8* exons 1 to 7 are indicated

as blue vertical bars above the array-CGH chart. The x and y axes represent genomic coordinates and the log₂ hybridization signals, respectively (Color figure online)

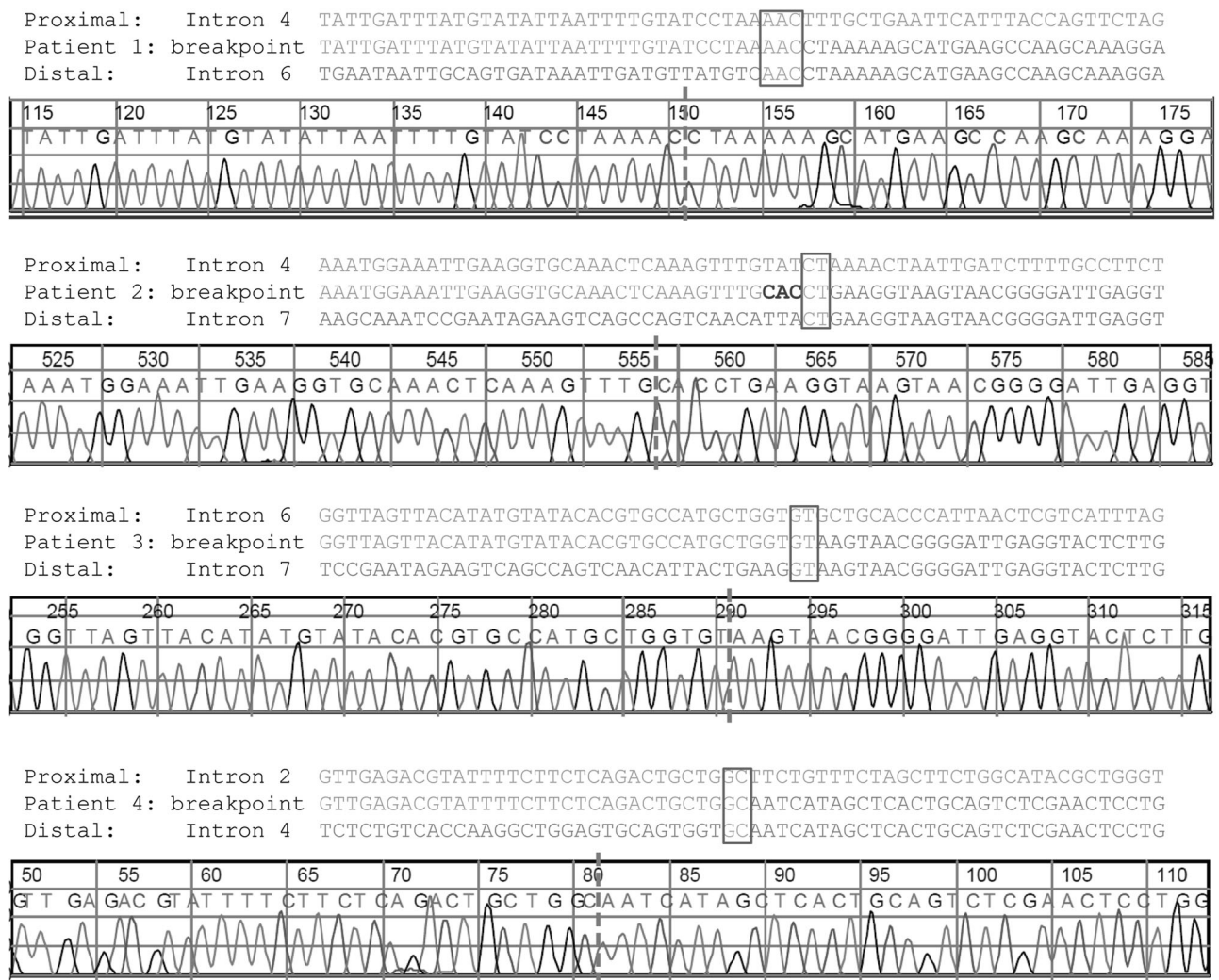


Fig. 4 Breakpoint sequence analysis of the *HDAC8* deletions. DNA sequences were aligned to the normal wild-type proximal and distal sequences. Sequence homology to the normal proximal and distal

wild-type sequences are shown in green and red. Boxed sequences (blue) indicate regions of microhomology and dash red lines reveal the breakpoint junctions (Color figure online)

The proximal breakpoint for Subject 3 lies within a long interspersed repeat element (LINE; *LIPA3*) and shows a two base-pair microhomology (GT) at the breakpoint junction (Fig. 4c). The distal deletion breakpoint of Subject 4 maps to a short interspersed repeat element (SINE; *AluJr*) and has a two base-pair microhomology (GC) at the breakpoint junction (Fig. 4d).

Discussion

We describe the identification of four novel intragenic deletions in the *HDAC8* gene, uncovering a genetic etiology in ~3% of individuals in this cohort. All Subjects presented with clinical features consistent with CdLS/atypical CdLS (Table 1, Fig. 1). The deletions range in size from 2.4 to 70 kb, encompass up to three exons and appear to be novel to

this study supporting the broad allelic heterogeneity of *HDAC8* mutations in CdLS (Fig. 2).

To date, six gross deletions and one insertion in *HDAC8* have been reported [13], however no insights have been provided into the developmental mechanisms of these rearrangements. This prompted us to characterize deletion breakpoints molecularly and examine the breakpoint regions. Interestingly, we uncovered the presence of two to three base-pairs of microhomology at the breakpoints in all cases (Fig. 4). Furthermore, analysis of the sequences surrounding the breakpoints revealed that in all cases the rearrangements occurred in, or in the proximity of, repetitive elements that are known to increase the genomic instability in certain regions [22]. The features observed at the breakpoint junctions for these cases suggest that a replication-based repair mechanism such as FoSTeS/MMBIR [16, 17] could underlie a proportion of these

rearrangements in *HDAC8*, similar to what has been already proposed for intragenic copy number aberrations in the *NIPBL* gene [23]. The presence of microhomology at the breakpoints in all cases argues against a NHEJ mechanism. Furthermore, the insertion-deletion of the three base-pair CAC sequence in Subject 2 indicates that at least one additional template-switch occurred to acquire this unique sequence, and strongly supports a FoSTeS/MMBIR mechanism.

Somatic mosaicism in *NIPBL* has been described in multiple patients with CdLS. In a proportion of patients, the mutation is identifiable only in buccal samples and is undetectable in blood [8]. Mosaicism has also been reported in *SMC1A* and *SMC3* [8, 12]. To our knowledge, the mosaic case reported herein is the first described patient with a mosaic *HDAC8* mutation associated with clinical features of CdLS. Only one other case of somatic mosaicism for an *HDAC8* variant has been reported in the apparently unaffected mother of two patients with *HDAC8*-related CdLS [14]. Quantitative PCR analysis indicated that in this Subject ~38% of blood lymphocytes and nearly all buccal cells contained the deletion. A comparison of the provided clinical features (Table 1) did not seem to suggest a significant difference in the severity of the phenotype of Subject 4 versus other patients possibly suggesting that the mosaicism cannot mitigate the phenotypic impact of a damaging mutation. In addition, because testing was only performed in peripheral blood and buccal cells, the results may not accurately reflect the mutation load in other tissues.

The *HDAC8* mosaic deletion reported here again highlights the fact that the prevalence of somatic mosaicism in the CdLS-associated genes could be underestimated, as many of these cases may remain undetected. Given that mosaicism in other CdLS genes is not infrequent, it is likely that a proportion of patients included in this study have somatic mosaicism in any of the five-known CdLS genes but Sanger sequencing and array-CGH failed to identify a mutation in DNA isolated from blood. The use of more sensitive techniques, such as targeted analysis of the five CdLS genes by deep next generation sequencing of DNA isolated from blood and/or buccal cells is likely to be available in clinical diagnostic settings in the near future.

All Subjects exhibited skewed X-inactivation, consistent with previous reports [13, 14]. Subjects 1, 2 and 3 exhibited highly skewed X-inactivation in blood. Subject 4, who is mosaic for a deletion of exons 3 and 4, exhibited an X-inactivation ratio consistent with random inactivation in her blood sample and moderately skewed X-inactivation in buccal cells. While this patient's deletion was detectable in blood, the presence of the deletion was more clearly demonstrated in buccal cells, suggesting a higher proportion of cells harboring the mutated allele in this cell lineage.

Although X-inactivation studies are not able to distinguish which allele is preferentially inactivated, the observation that the sample with a higher proportion of deleted alleles has increased X-inactivation skewing suggests that the X chromosome with the *HDAC8* deletion is likely to be preferentially inactivated.

In conclusion, this study identifies additional underlying causes of CdLS, describes the first instance of a somatic *HDAC8* mutation in an individual with CdLS features and provides insight into the molecular bases of *HDAC8* deletions. The frequency of the deletions identified in this cohort highlights the importance of utilizing multiple techniques including copy number analysis of *HDAC8* in individuals with a suspected diagnosis of CdLS who are negative for mutations in other CdLS-associated genes. Finally, the identification of a somatic mutation in *HDAC8* suggests that the analysis of DNA derived from buccal cells should be considered to investigate whether a patient may have a somatic mosaicism if lymphocyte analysis has failed to identify a mutation.

Compliance with ethical standards

Conflict of interest The authors declare that they have no conflict of interest.

References

1. Kline AD, Krantz ID, Sommer A, Kliever M, Jackson LG, FitzPatrick DR, et al. Cornelia de Lange syndrome: clinical review, diagnostic and scoring systems, and anticipatory guidance. *Am J Med Genet A*. 2007;143A:1287–96.
2. Rohatgi S, Clark D, Kline AD, Jackson LG, Pie J, Siu V, et al. Facial diagnosis of mild and variant CdLS: Insights from a dysmorphologist survey. *Am J Med Genet A*. 2010;152A:1641–53.
3. Krantz ID, McCallum J, DeScipio C, Kaur M, Gillis LA, Yaeger D, et al. Cornelia de Lange syndrome is caused by mutations in *NIPBL*, the human homolog of *Drosophila melanogaster* Nipped-B. *Nat Genet*. 2004;36:631–35.
4. Deardorff MA, Kaur M, Yaeger D, Rampuria A, Korolev S, Pie J, et al. Mutations in cohesin complex members *SMC3* and *SMC1A* cause a mild variant of cornelia de Lange syndrome with predominant mental retardation. *Am J Hum Genet*. 2007;80:485–94.
5. Musio A, Selicorni A, Focarelli ML, Gervasini C, Milani D, Russo S, et al. X-linked Cornelia de Lange syndrome owing to *SMC1L1* mutations. *Nat Genet*. 2006;38:528–30.
6. Deardorff MA, Wilde JJ, Albrecht M, Dickinson E, Tennstedt S, Braunholz D, et al. *RAD21* mutations cause a human cohesinopathy. *Am J Hum Genet*. 2012;90:1014–27.
7. Deardorff MA, Bando M, Nakato R, Watrin E, Itoh T, Minamino M, et al. *HDAC8* mutations in Cornelia de Lange syndrome affect the cohesin acetylation cycle. *Nature*. 2012;489:313–17.
8. Huisman SA, Redeker EJ, Maas SM, Mannens MM, Hennekam RC. High rate of mosaicism in individuals with Cornelia de Lange syndrome. *J Med Genet*. 2013;50:339–44.
9. Nizon M, Henry M, Michot C, Baumann C, Bazin A, Bessieres B, et al. A series of 38 novel germline and somatic mutations of

- NIPBL in Cornelia de Lange syndrome. *Clin Genet*. 2016;89:584–89.
10. Baquero-Montoya C, Gil-Rodríguez MC, Braunholz D, Teresa-Rodrigo ME, Obieglo C, Gener B, et al. Somatic mosaicism in a Cornelia de Lange syndrome patient with NIPBL mutation identified by different next generation sequencing approaches. *Clin Genet*. 2014;86:595–97.
 11. Rohlin A, Wernersson J, Engwall Y, Wiklund L, Bjork J, Nordling M. Parallel sequencing used in detection of mosaic mutations: comparison with four diagnostic DNA screening techniques. *Hum Mutat*. 2009;30:1012–20.
 12. Ansari M, Poke G, Ferry Q, Williamson K, Aldridge R, Meynert AM, et al. Genetic heterogeneity in Cornelia de Lange syndrome (CdLS) and CdLS-like phenotypes with observed and predicted levels of mosaicism. *J Med Genet*. 2014;51:659–68.
 13. Kaiser FJ, Ansari M, Braunholz D, Concepción Gil-Rodríguez M, Decroos C, Wilde JJ, et al. Loss-of-function HDAC8 mutations cause a phenotypic spectrum of Cornelia de Lange syndrome-like features, ocular hypertelorism, large fontanelle and X-linked inheritance. *Hum Mol Genet*. 2014;23:2888–900.
 14. Parenti I, Gervasini C, Pozojevic J, Wendt KS, Watrin E, Azzollini J, et al. Expanding the clinical spectrum of the 'HDAC8-phenotype' - implications for molecular diagnostics, counseling and risk prediction. *Clin Genet*. 2016;89:564–73.
 15. Inoue K, Lupski JR. Molecular mechanisms for genomic disorders. *Annu Rev Genomics Hum Genet*. 2002;3:199–42.
 16. Zhang F, Gu W, Hurles ME, Lupski JR. Copy number variation in human health, disease, and evolution. *Annu Rev Genomics Hum Genet*. 2009;10:451–81.
 17. Lee JA, Carvalho CM, Lupski JRA. DNA replication mechanism for generating nonrecurrent rearrangements associated with genomic disorders. *Cell*. 2007;131:1235–47.
 18. Hastings PJ, Ira G, Lupski JR. A microhomology-mediated break-induced replication model for the origin of human copy number variation. *PLoS Genet*. 2009;5:e1000327.
 19. Livak KJ, Schmittgen TD. Analysis of relative gene expression data using real-time quantitative PCR and the 2(-Delta Delta C(T)) method. *Methods*. 2001;25:402–8.
 20. Corpet F. Multiple sequence alignment with hierarchical clustering. *Nucleic Acids Res*. 1988;16:10881–90.
 21. Allen RC, Zoghbi HY, Moseley AB, Rosenblatt HM, Belmont JW. Methylation of HpaII and HhaI sites near the polymorphic CAG repeat in the human androgen-receptor gene correlates with X chromosome inactivation. *Am J Hum Genet*. 1992;51:1229–39.
 22. Argueso JL, Westmoreland J, Mieczkowski PA, Gawel M, Petes TD, Resnick MA. Double-strand breaks associated with repetitive DNA can reshape the genome. *Proc Natl Acad Sci USA*. 2008;105:11845–50.
 23. Pehlivan D, Hullings M, Carvalho CM, Gonzaga-Jauregui CG, Loy E, Jackson LG, et al. NIPBL rearrangements in Cornelia de Lange syndrome: evidence for replicative mechanism and genotype-phenotype correlation. *Genet Med*. 2012;14:313–22.